Intensity and Lifetime Ratiometric Luminescent Thermometer based on a Tb(III) Coordination Polymer

Augusto Iwashita Costa,[a] Rafaela M.R. da Silva,[a] Luckerman D.G. Botelho,[a] Sergio F.N. Coelho,[b] Fernando Sigoli,[b] João H. de Araujo-Neto,[c] Javier Ellena,[c] Felipe T. Martins,[d] Angelo M.S. Gomes,[e] Wallace C. Nunes,[f] Francesc Lloret,[g] Miguel Julve,[g] and Maria Vanda Marinho.[a*]

[a]Instituto de Química, Universidade Federal de Alfenas, Campus Santa Clara, Alfenas, MG, 37133-840, Brazil.

[b]Instituto de Química, Universidade Estadual de Campinas, Cidade Universitária, Campinas, SP 13083-970, Brazil.

[c]Instituto de Física, Universidade de São Paulo, São Carlos, SP 13566-590, Brazil.

[d]Instituto de Física, Universidade Federal de Goiás, Campus Samambaia, Goiânia, GO 74690-900, Brazil.

[e]Instituto de Física, Universidade Federal do Rio de Janeiro, Cidade Universitária, Rio de Janeiro 21941-972, Brazil

[f]Instituto de Física, Universidade Federal Fluminense, Rio de Janeiro, RJ 24210-346, Brazil.

[g]Instituto de Ciencia Molecular (ICMol)/Departament de Química Inorgànica, Universitat de València, 46980 Paterna, València, Spain.

*E-mail: *maria.marinho@unifal-mg.edu.br*

Table S1. Selected data about the coordination networks based on deprotonated forms of the H_4bttb and H_2-2,5-pzdc acids in the last decade (2012-2022) and this year (2023)*

H_4bttb						
Formulae*	Metal Ion/ CN	Experimental Approach	Coordination mode of the carboxylate group	Database Identifier	Ref.	Year
$\{[Ni\text{-}(H_2bttb)(H_2O)_2]\cdot 2DIOX\}_n$	$Ni^{II}/6$	Solvothermal 100 °C - 4 days	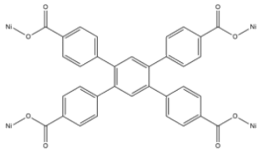	MIFMIZ	1	2013
$\{[Zn(H_2bttb)]\cdot 3DEF\cdot 2H_2O\}_n$	$Zn^{II}/6$	Solvothermal 100 ºC - 4 days	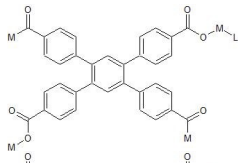	MIFBAG, MIFJOC	1	2013
$\{[Mg(H_2bttb)(C_2H_5OH)_2]\cdot 4DEF\}_n$	$Mg^{II}/6$	Solvothermal 100 ºC - 4 days	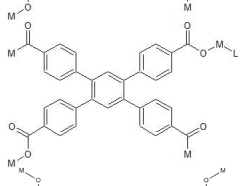	MIFBEK, MIFKIX	1	2013
$[M(bttb)_{0.5}(DMBPY)_{0.5}]_n$	$Co^{II}/5$	Solvothermal 100 °C - 4 days	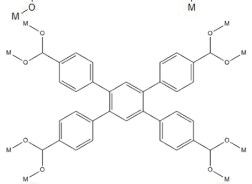	ONULOA	2	2014
$[Ce(Hbttb)\cdot(EtOH)_{0.28}(H_2O)_{2.75}]_n$	$Ce^{III}/9$	Solvothermal	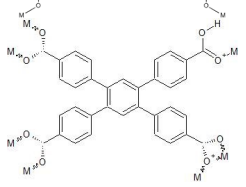	FOFCIO	3	2014

$[Nd(Hbttb)\cdot(EtOH)_{0.28}(H_2O)_{2.75}]_n$	$Nd^{III}/9$	Solvothermal	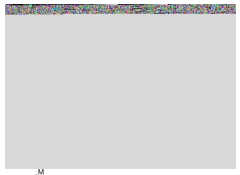	FOCYUT	3	2014
$\{[Co_3(\mu_6\text{-bttb})(\mu_4\text{-}H_2bttb)(ade)_2]\cdot H_2O\}_n$	$Co^{II}/5$	Hydrothermal (water) 100 °C - 2 days	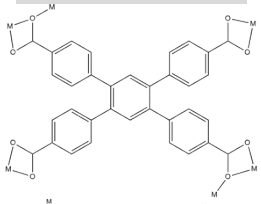	QUFKEJ	4	2015
$(C_{34}H_{20}CaO_8)_n\cdot 2.66(H_2O)$	$Ca^{II}/6$	-	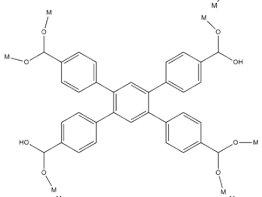	YUNJIC	5	2015
$(C_{34}H_{20}CaO_8)_n$	$Ca^{II}/6$	-	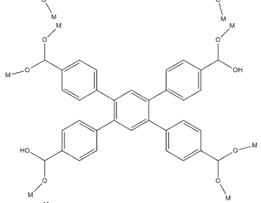	YUNJOI	5	2015
$(C_{34}H_{20}CaO_8)_n\cdot 1.45(Xe)$	$Ca^{II}/6$	-	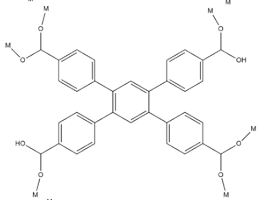	YUNJUO	5	2015
$(C_{34}H_{20}CaO_8)_n\cdot 0.51(Kr)$	$Ca^{II}/6$	-	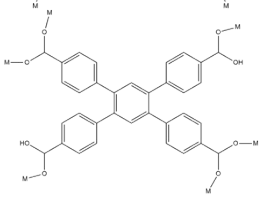	YUNKAV	5	2015

$[Zn_2(bttb)(BPDPNDI)]$	$Zn^{II}/5$	(DMF) 80 °C – 24 hr	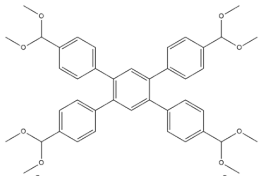	DUNPEJ	[6]	2015
$\{[Cd_3(Hbttb)_2 \cdot (H_2O)_2] \cdot (DEF)_4(H_2O)_6\}_n$ CdBTTB[b]	$Cd^{II}/6$	Solvothermal	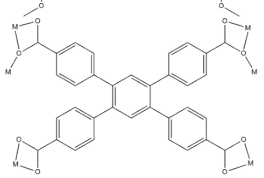	GOSDEZ	[7]	2015
$\{[Zn_6(bttb)_3(H_2BDC)(H_2O)_4] \cdot (DEF)\}_n$ ZnBTTBBDC[b]	$Zn^{II}/6$	Solvothermal	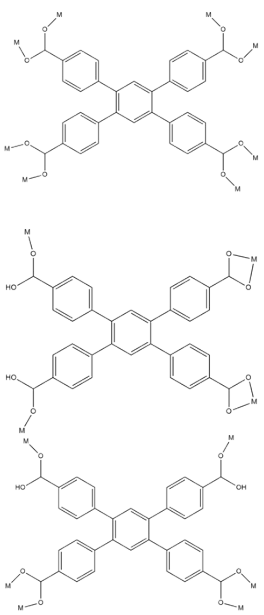	GOSDID	[7]	2015

$\{[Co_2(bttb)\cdot(BPY)]\cdot(H_2O)(DEF)_2\}_n$ CoBTTBBPY[b]	Co^{II}/6	Solvothermal	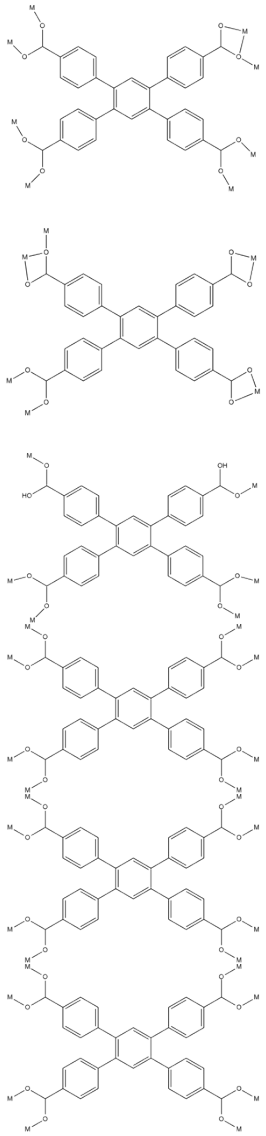	GOSDOJ	[7]	2015
$\{[Zn_2(bttb)\cdot(BPY)]\cdot(DEF)_2\}_n$ ZnBTTBBPY[b]	Zn^{II}/5	Solvothermal		GOSDUP	[7]	2015
$\{[Co_2(bttb)\cdot(AZPY))]\cdot(DEF)_2\}_n$ CoBTTBAZPY[b]	Co^{II}/6	Solvothermal		GOSFAX	[7]	2015

$\{[Cd_2(bttb)(H_2O)_5]\cdot 3H_2O\}_n$	$Cd^{II}/4$	Solvothermal 110 ºC - 3 days	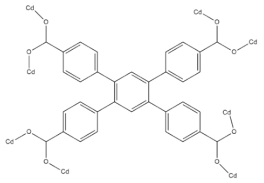	ESECUC	[8]	2016
$\{[Zn_2(bttb)]\cdot 5H_2O\}_n$	$Zn^{II}/4$	Solvothermal 110 ºC - 3 days	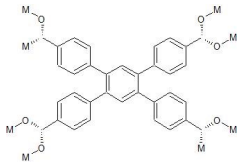	ESEDAJ	[8]	2016
$\{[Mn_2(bttb)(H_2O)_5]\cdot 2H_2O\}_n$	$Mn^{II}/4$	Solvothermal 130 ºC - 3 days	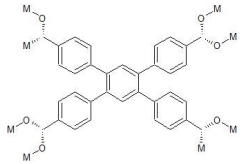	ESEDEN	[8]	2016
$\{[Zr_6(\mu_3\text{-}O)_4(\mu_3\text{-}OH)_4(OH)_4(H_2O)_4(bttb)_2]\}_n$ M-CAU-24[b]	Zr^{IV}/ Ce^{IV}	Stirring 100 °C – 15 min	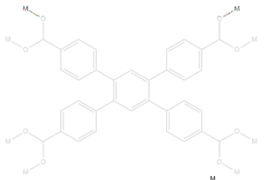	IZIBUQ	[9]	2016
$[Ca(H_2bttb)_n\cdot (C_2H_2)_{1.76}$ SBMOF-2:C_2H_2[b]	$Ca^{II}/6$	Solvothermal 100 ºC - 3 days	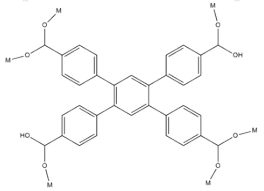	OKAYOQ	[10]	2016

$[Ca(H_2bttb)_n \cdot (C_2H_4)_{1.47}$ SBMOF-2:C_2H_4[b]	Ca^{II}/6	Solvothermal 100 ºC - 3 days	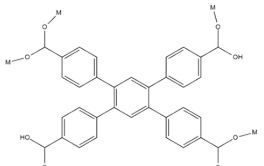	OKAYUW	[10]	2016
$[Ca(H_2bttb)_n \cdot (C_2H_6)_{1.58}$ SBMOF-2:C_2H_6[b]	Ca^{II}/6	Solvothermal 100 ºC - 3 days	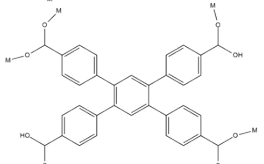	OKAZAD	[10]	2016
$\{[Cd(H_2bttb)] \cdot 5H_2O\}_n$	Cd^{II}/8	Solvothermal 180 ºC - 3 days	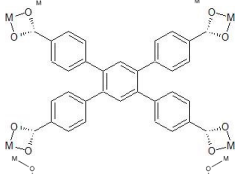	FENHIS	[11]	2017
$\{\|DMA\|_3[Y_9(\mu_3\text{-}O)_2(\mu_3\text{-}OH)_{12}(OH)_2(H_2O)_7(bttb)_3] \cdot (solv)_x\}_n$	Y^{III}	Solvothermal	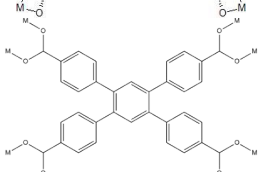	HEJFUA	[12]	2017
Y-shp-MOF-5[b]						
Y-shp-MOF-5 (0% RH)	Y^{III}	Solvothermal	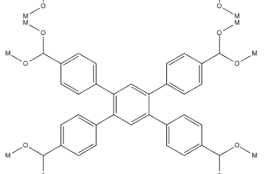	HEJGAH	[12]	2017
Y-shp-MOF-5 22% humidity	Y^{III}	Solvothermal	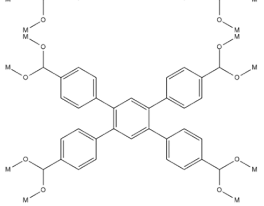	HEJGEL	[12]	2017

Y-shp-MOF-5 100% humidity	Y^{III}	Solvothermal	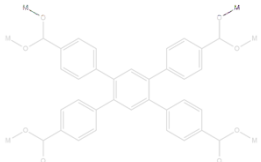	HEJGIP	[12]	2017
$[Zn_2(bttb)(L2)]\cdot 2DMF$	$Zn^{II}/5$	Solvothermal 80 °C – 48 hr	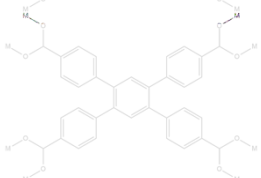	OCINAS	[13]	2017
$[Co_2(bttb)(L2)(H_2O)(\mu\text{-}H_2O)(DMF)]\cdot 2.7DMF$	$Co^{II}/6$	Solvothermal 80 °C – 48 hr	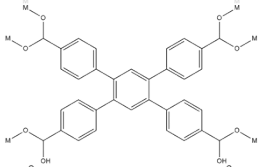	OCINEW	[13]	2017
$[Cd(H_2bttb)]_n\cdot 0.5nH_2O$	$Cd^{II}/8$	Solvothermal 180 °C – 72 hr	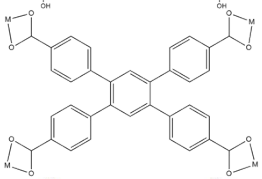	FENHIS	[14]	2018
$\{[Bi_2(H_2bttb)(bttb)(H_2O)_2]\cdot xH_2O\}_n$	$Bi^{III}/8$	Solvothermal 80 ºC - 12 hr	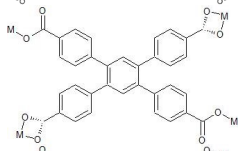	MIHMEY	[15]	2018
$\{H_2N(CH_3)_2[Bi(bttb)(H_2O)]\cdot xH_2O\}_n$	$Bi^{III}/9$	Solvothermal 100 ºC - 12 hr	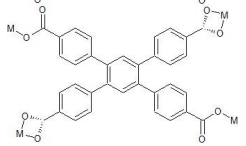	MIHMIC	[15]	2018
$\{[Bi_4(O)_2(OH)_2(H_2bttb)(bttb)(H_2O)_2]\cdot x H_2O\}_n$	$Bi^{III}/5$	Solvothermal 120 ºC - 12 hr		MIHMOI	[15]	2018

			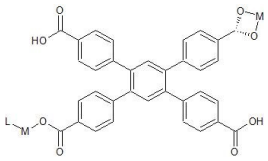			
$[Ca(bttb]_n \cdot 1.2n(I_2)$ I_2@SBMOF-2[b]	Ca^{II}/6	Solvothermal	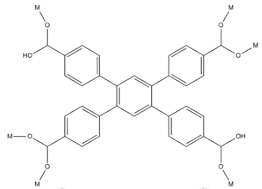	OFOQUY	16	2018
$\{[Co(bttb)_{0.5}(H_2O)]\cdot DMF\}_n$	Co^{II}/6	Solvothermal 85 ºC - 4 days	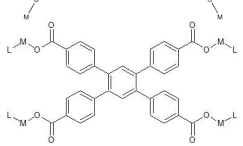	FIYDEZ	17	2019
$[C_{34}O_8H_{18}]_3(F/OH)_6(H_2O)_{18}(NpO_2)_{18}$	Np^{V}/7	Solvothermal 130 °C – 72 hr	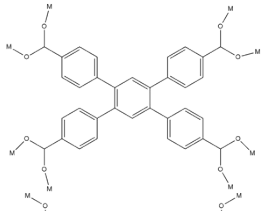	VOPGAL	18	2019
$[Sc_2(OH)_2(bttb)]$	Sc^{III}/6	Solvothermal 170 °C – 48 hr	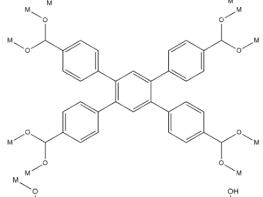	SUMBAG	19	2020
$\{Zn(cyclam)(H_2bttb)(DMF)_2]\}_n$ IRH-5-as synthesized[b]	Zn^{II}/6	Solvothermal 90 °C - 3 days	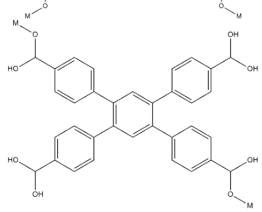	ATICEO	20	2021

$\{Cu(cyclam)(H_2bttb)(DMF)_2]\}_n$ IRH-4-as synthesized[b]	$Cu^{II}/6$	Solvothermal 90 °C - 3 days	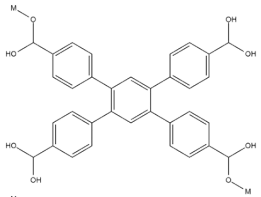	ATICUE	[20]	2021
IRH-5-dichloromethane[b]	$Zn^{II}/6$	Solvothermal 90 °C - 3 days	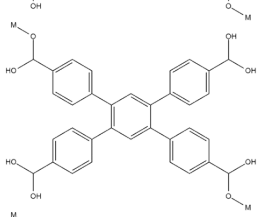	ATIBUD	[20]	2021
IRH-5-activated[b]	$Zn^{II}/6$	Solvothermal 90 °C - 3 days	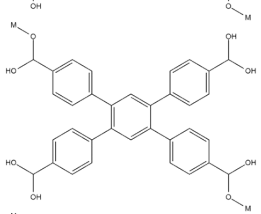	ATICAK	[20]	2021
IRH-4-activated[b]	$Cu^{II}/6$	Solvothermal 90 °C - 3 days	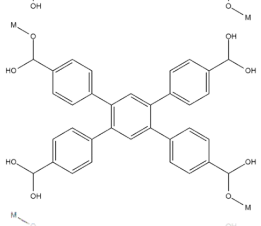	ATICIS	[20]	2021
IRH-4-dichloromethane[b]	$Cu^{II}/6$	Solvothermal 90 °C - 3 days	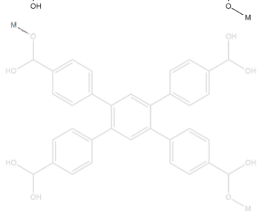	ATICOY	[20]	2021
$[In_2(bttb)(OH)_2]$	$In^{III}/6$	Solvothermal 100 °C – 48 hr	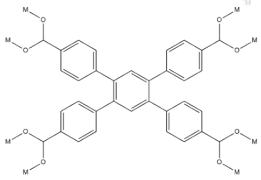	ODAXEA	[21]	2021

$[Ce(Hbttb)(PO)]_n$	Ce^{III}	Solvothermal 120°C- 2 days/ Loading with propylene oxide (PO)	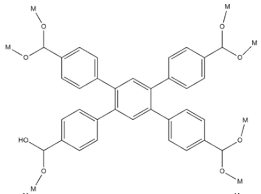	LARPAZ	[22]	2022
$\{[(Yb_6(\mu_3\text{-}OH^-)_8(H_2O)_4(OH^-)_2][(Nd_6(\mu_3\text{-}OH^-)_4(\mu_3\text{-}O)_2(H_2O)_6(OH^-)_2]\}$ YbNdTCPB[b]	Yb^{III}/7 Nd^{III}/6	115 °C - 18 hr	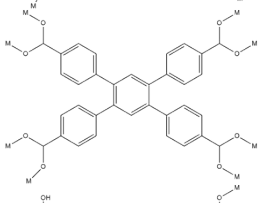	GIHVUS	[23]	2022
$\{[(CH_3)_2NH_2][Eu(bttb)(H_2O)_2]\cdot DMF\}_n$	Eu^{III}/8	Solvothermal 120 °C - 3 days	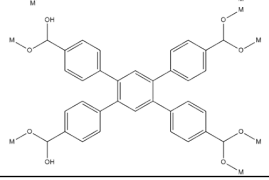	JIFDUB	[24]	2023

[a]Abbreviations: CN: coordination number; H_4bttb = 1,2,4,5-tetrakis(4'-carboxyphenyl)benzene; DIOX = dioxane, DMF= dimethylformamide; DMBPY: 2,2'-dimethyl-4,4'-bipyridine; DEF = N,N'-diethylformamide; PO = propylene oxide; DMA = dimethylammonium cation, solv = solvent; cyclam = 1,4,8,11-tetraazacyclotetradecane; BDC = 1,4-benzenedicarboxylic acid; BPY = bipyridine; AZPY = azopyridine; IRH = Institut de Recherche sur l'Hydrogène; shp = square hexagonal-prism; RH = relative humidity; L2= 1,7-bis{(pyridin-4'-yl)methanol}-1,7-dicarba-closo-dodecaboranes; CAU = Christian-Albrechts-University; BPDPNDI = N,N'--bis(4-pyridyl)-2,6-dipyrrolidyl naphthalenediimide. [b]: as denoted in the reference paper.

H_2-2,5-pzdc						
Formulae*[a]	Metal Ion/CN	Experimental Approach	Coordination mode of the carboxylate group	Database Identifier	Ref.	Year
$[Ce(2,5\text{-pzdc})_{1.5}(H_2O)]_n$	Ce^{III}/9	Solvothermal 160 ºC - 3 days	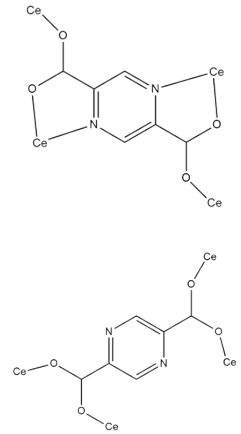	NATXEN	25	2012
$\{[Er(2,5\text{-pzdc})(\mu\text{-}OH)(H_2O)]\cdot H_2O\}_n$	Er^{III}/8	Solvothermal 160 ºC - 3 days	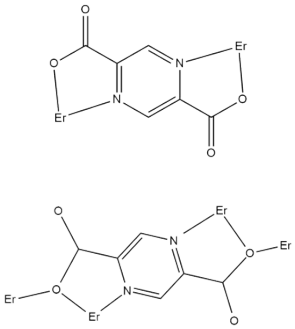	NATXIR	25	2012

$\{[Tm(2,5\text{-pzdc})_{1.5}(\mu_4(H_2O)_2]\cdot 3H_2O\}_n$	$Tm^{III}/9$	Solvothermal - 150 ºC-1 day	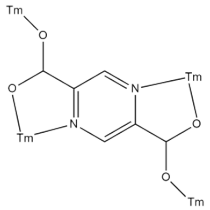	FEDBEX	[26]	2012
$\{[La(2,5\text{-pzdc})(NO_3)(H_2O)_2]\cdot 2.33H_2O\}_n$	$La^{II}/10$	Mechanochemical 150 ºC - 3 days	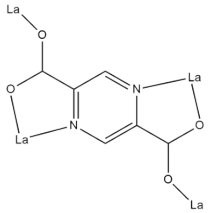	BUSSAL	[27]	2015
$\{[Ce(2,5\text{-pzdc})(NO_3)(H_2O)_2]\cdot 2.33H_2O\}_n$	$Ce^{III}/10$	Mechanochemical 150 ºC - 3 days	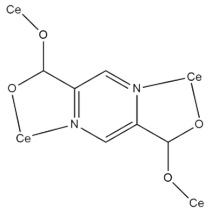	-	[27]	2015
$\{[Pr_9(2,5\text{-pzdc})_9(NO_3)_2(H_2O)_{25}](NO_3)_7\cdot 8H_2O\}n$	$Pr^{III}/9$	Mechanochemical; 130 ºC-3 days	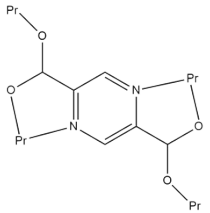	BUSTAM	[27]	2015

$\{[Nd_9(2,5\text{-pzdc})_9(NO_3)_2(H_2O)_{25}](NO_3)_7\cdot 8H_2O\}_n$	$Nd^{III}/9$	Mechanochemical; 130 ºC-3 days	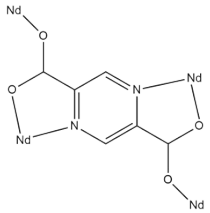	BUSSEP	[27]	2015
$\{[Nd_6(2,5\text{-pzdc})_8(H_2O)_{10}]\ (NO_3)_2\cdot 2H_2O\}_n$	$Nd^{III}/9$	Mechanochemical; 150-170 ºC-3 days	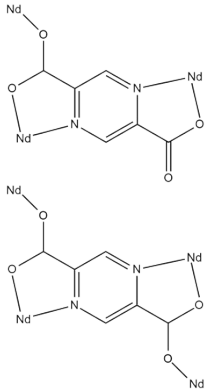	BUSSIT	[27]	2015
$\{[Sm_6(2,5\text{-pzdc})_8(H_2O)_{10}]\ (NO_3)_2\cdot 2H_2O\}_n$	$Sm^{III}/9$	Mechanochemical; 150-170 ºC-3 days	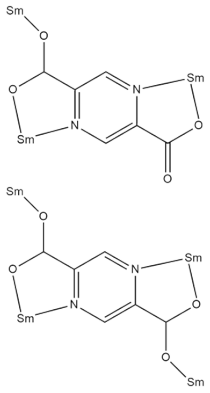	-	[27]	2015

$[Eu(2,5\text{-pzdc})(NO_3)(H_2O)]_n$	Eu^{III}/9)	Mechanochemical; 180 ºC-3 days	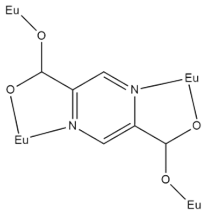	BUSSOZ	[27]	2015
$[Gd(2,5\text{-pzdc})(NO_3)(H_2O)]_n$	Gd^{II}/9	Mechanochemical; 180 ºC- 3 days	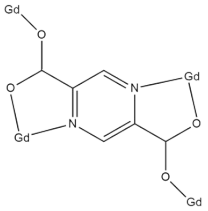	-	[27]	2015
$[Tb(2,5\text{-pzdc})(NO_3)(H_2O)]_n$	Tb^{III}/9	Mechanochemical; 180 ºC- 3 d	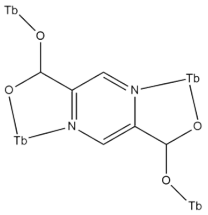	BUSSUF	[27]	2015
$\{[Ce_2(2,5\text{-pzdc})_3(H_2O)_4]\cdot 6H_2O\}_n$	Ce^{III}/9	Hydrothermal 170 ºC - 3 days	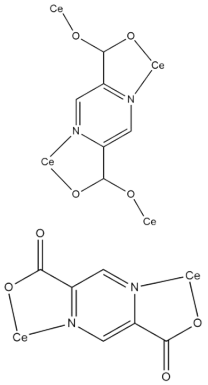	VASFAZ	[28]	2017

$\{[Pr_2(2,5\text{-pzdc})_3(H_2O)_4]\cdot 6H_2O\}_n$	Pr^{III}/9	Hydrothermal 170 ºC - 3 days	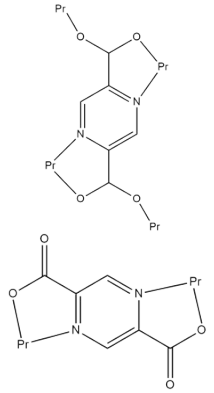	VASFED	[28]	2017
$\{[Nd_2(2,5\ pzdc)_3(H_2O)_4]\cdot 6H_2O\}_n$	Nd^{III}/9	Hydrothermal 170 ºC - 3 days	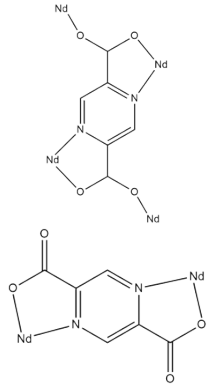	VASFON	[28]	2017
$\{[Eu(2,5\text{-pzdc})_3(H_2O)_4]\cdot 6H_2O\}_n$	Eu^{III}/9	Hydrothermal 170 ºC - 3 days	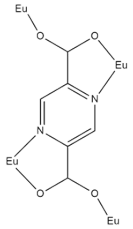	VASFUT	[28]	2017

$\{[Er_2(2,5\text{-pzdc})_3(H_2O)_4]\cdot 5H_2O\}_n$	$Er^{III}/9$	Hydrothermal 170 ºC - 3 days	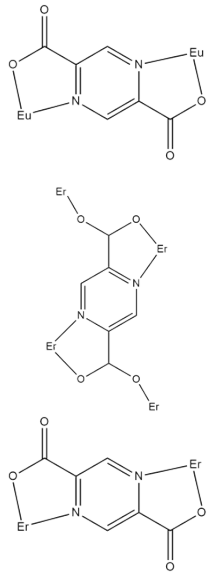	VASFIH	[28]	2017
$[La_2(H_2O)_2(NMP)_2(2,5\text{-pzdc})_3]_n$	$La^{III}/9$	Solvothermal 100 ºC - 1 day	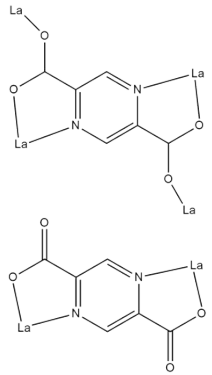	ZUZKAJ	[29]	2020

$[Ce_2(H_2O)_2(NMP)_2(2,5\text{-}pzdc)_3]_n$	Ce^{II}/9	Solvothermal 100 ºC - 1 day	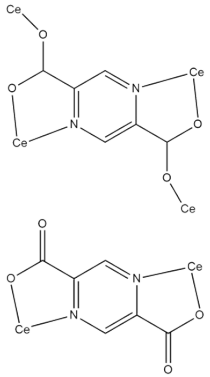	-	[29]	2020
$[Pr_2(H_2O)_2(NMP)_2(2,5\text{-}pzdc)_3]_n$	Pr^{III}/9	Solvothermal 100 ºC - 1 day	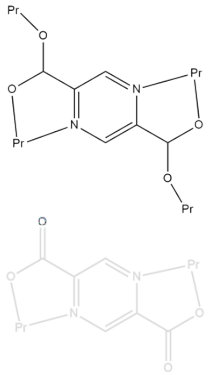	-	[29]	2020
$[Nd_2(H_2O)_2(NMP)_2(2,5\text{-}pzdc)_3]_n$	Nd^{III}/9	Solvothermal 100 ºC - 1 day	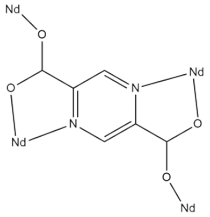	-	[29]	2020

$[Sm_2(H_2O)_2(NMP)_2(2,5\text{-}pzdc)_3]_n$	$Sm^{III}/9$	Solvothermal 100 ºC - 1 day	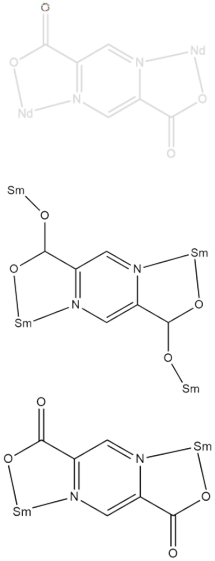	-	[29]	2020
$[Eu_2(H_2O)_2(NMP)_2(2,5\text{-}pzdc)_3]_n$	$Eu^{III}/9$	Solvothermal 100 ºC - 1 day	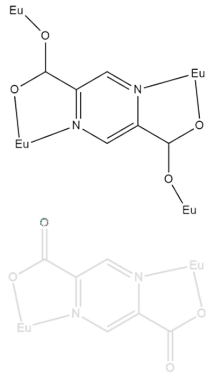	-	[29]	2020

$[Gd_2(H_2O)_2(NMP)_2(2,5\text{-pzdc})_3]_n$	$Gd^{III}/9$	Solvothermal 100 ºC -1 day	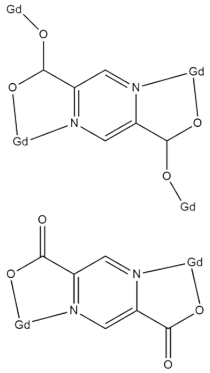	-	[29]	2020
$\{[Tb_2(H_2O)_4(2,5\text{-pzdc})_3]\cdot NMP\cdot 5H_2O\}_n$	$Tb^{III}/9$	Solvothermal 100 ºC - 1 day	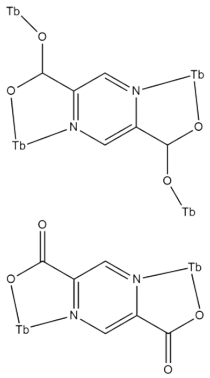	-	[29]	2020
$\{[Er_2(H_2O)_4(2,5\text{-pzdc})_3]\cdot NMP\cdot 5H_2O\}_n$	$Er^{III}/9$	Solvothermal 100 0ºC - 1 day	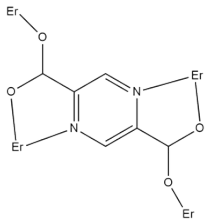	-	[29]	2020

$\{[Y_2(H_2O)_4(2,5\text{-pzdc})_3]\cdot NMP\cdot 5H_2O\}_n$	$Y^{III}/9$	Solvothermal 100 ºC - 1 day	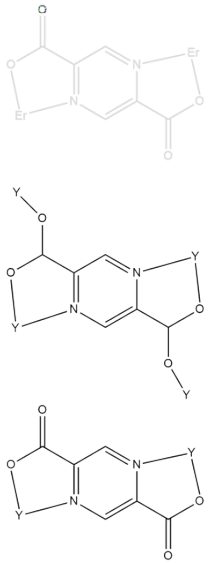	ZUZKEN	[29]	2020

*The revision for 2,5-pzdc^{2-} involved only coordination compounds with Ln^{III} ions. [a]Abbreviations: H_2-2,5-pzdc = 2,5-pyrazinedicarboxylic acid; NMP = ***N***-methyl-2-pyrrolidone.

Table S2. Main bond distances (Å) and angles (deg) for **1***

Tb1-O1	2.356(2)	Tb1- O5^{iv}	2.517(2)
Tb1- O1^{ii}	2.383(2)	Tb1- O6^{iv}	2.358(3)
Tb1-O3	2.279(3)	Tb1-N1	2.624(3)
Tb1- O4^{i}	2.305(3)	Tb1-Tb1^{i}	3.7557(2)
Tb1- O5^{iii}	2.381(2)	Tb1- Tb1^{ii}	3.7557(2)
O1 -Tb1 - O1^{i}	157.70(6)	O3 -Tb1 - O5^{iii}	119.20(12)
O1 -Tb1 - O5^{iii}	132.79(8)	O3 -Tb1 - O5^{iv}	73.60(11)
O1 -Tb1 - O5^{iv}	71.84(8)	O3 -Tb1 - O6^{iii}	73.16(12)
O1 ^{1}-Tb1 - O5^{iii}	69.01(7)	O3 -Tb1 - N1	124.01(11)
O1 -Tb1 - O6^{iii}	99.56(11)	O4 ^{i}-Tb1 - O1^{i}	95.49(11)
O1 ^{i}-Tb1 - N1	132.13(8)	O4 ^{i}-Tb1 - O5^{iii}	100.30(11)
O1 -Tb1 - N1	65.00(8)	O4 ^{i}-Tb1 - O5^{iv}	70.57(10)
O3 -Tb1 - O1^{i}	98.00(11)	O4 ^{i}-Tb1 - O6^{iii}	140.43(13)
O3 -Tb1 - O1	76.02(12)	O5 ^{iv}-Tb1 - O1^{i}	85.87(8)
O3 -Tb1 - O4^{i}	140.50(14)	O5 ^{iv}-Tb1 - O5^{iii}	152.64(7)
O6 ^{iii}-Tb1 - O5^{iv}	146.76(10)	O5 ^{iii}-Tb1 - N1	70.68(8)
O6 ^{iii}-Tb1 - O5^{iii}	52.81(9)	O6 ^{iii}-Tb1 - O1^{i}	99.13(12)
O6 ^{iii}-Tb1 - N1	75.46(13)	O1 -Tb1 - Tb1^{i}	156.01(6)

**Symmetry codes*: (i) = $-x + 3/2, y + 1/2, -z + 1/2$; (ii) = $-x + 3/2, y -1/2, -z + 1/2$; (iii) = $-x + 3/2, -y + 1/2, -z + 1$; (iv) = $x, -y, z - 1/2$; (v) = $-x + 3/2, -y + 1/2, -z$; (vi) = $-x + 1, -y + 1, -z + 1$; (vii) = $x, -y, z + 1/2$.

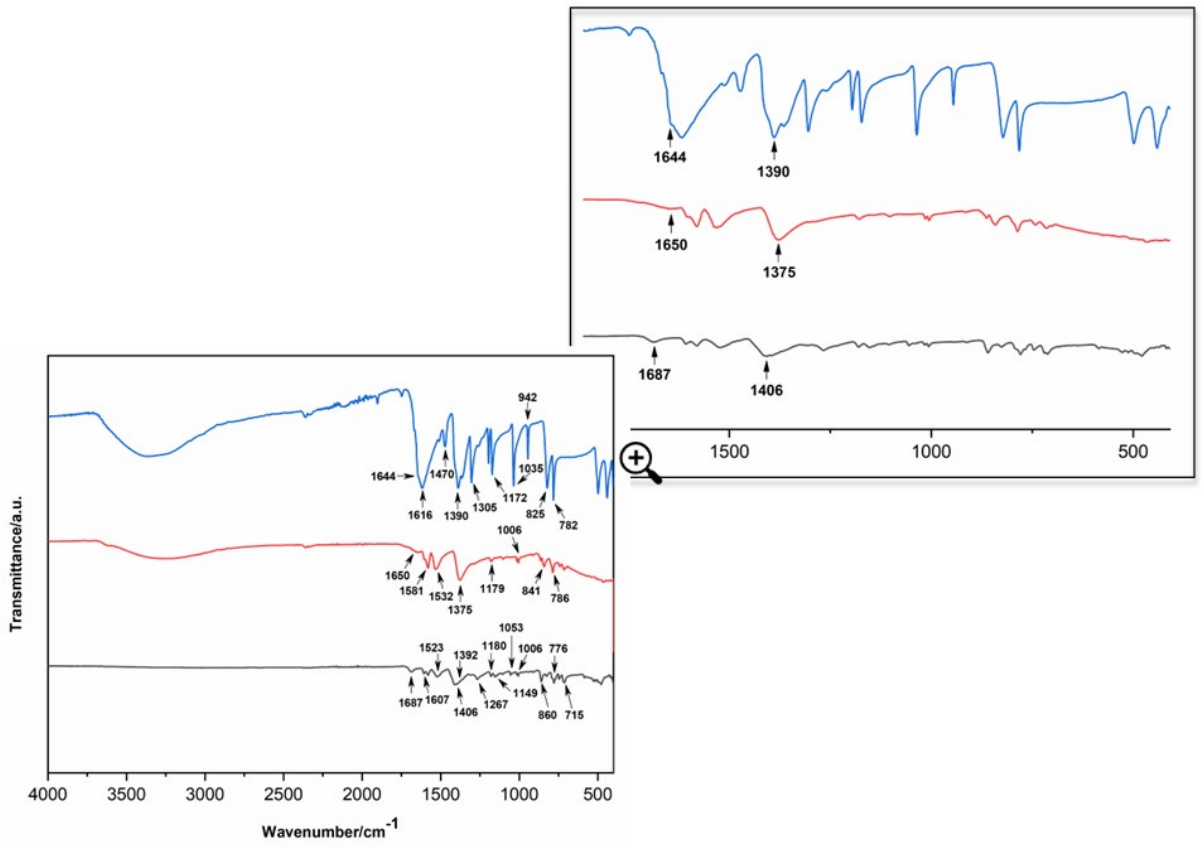

Figure S1. FTIR spectra of **1** (black trace), Na_4bttb (red trace), and $Na_2$2,5-pzdc salt (blue trace). The amplification shows the $\nu_{as}(COO^-)$ and $\nu_s(COO^-)$ stretching vibrations of the carboxylate groups aiming at getting a better visualization of $\Delta\nu$ in cm^{-1}.

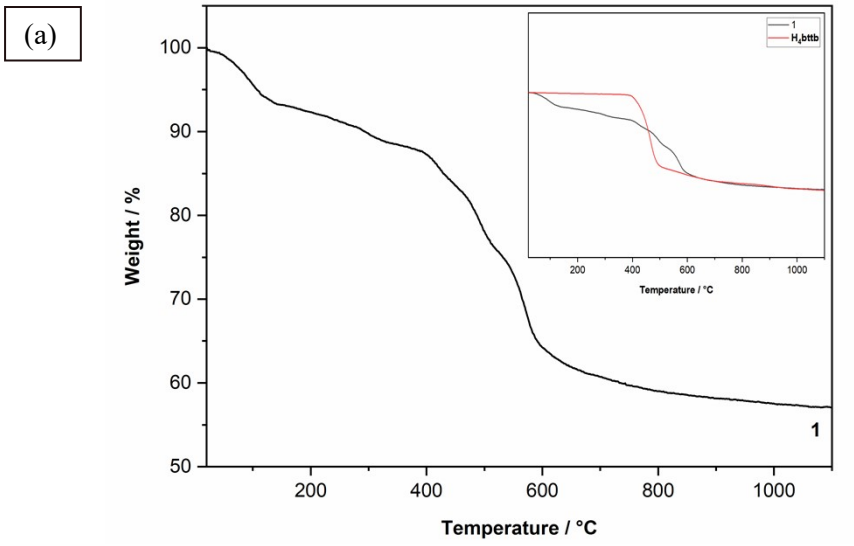

(b)

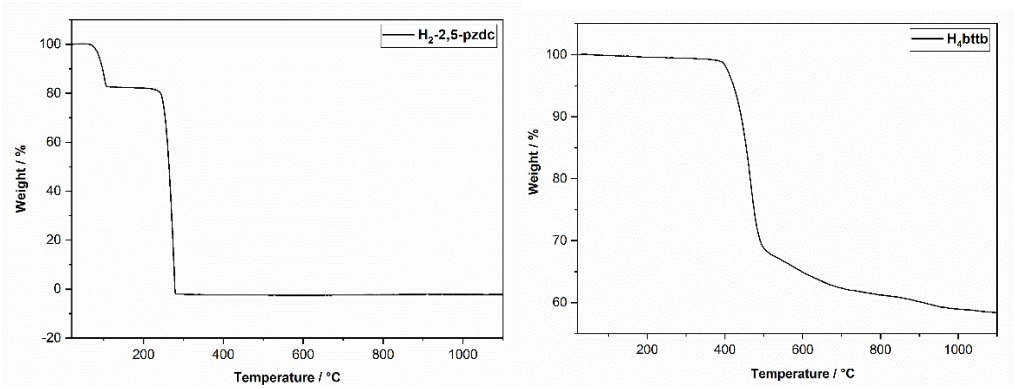

Figure S2. (a) TGA curve for **1** and TGA curves of **1** and H_4bttb (inside); (b) TGA curves for H_2-2,5-pzdc and H_4bttb acids.

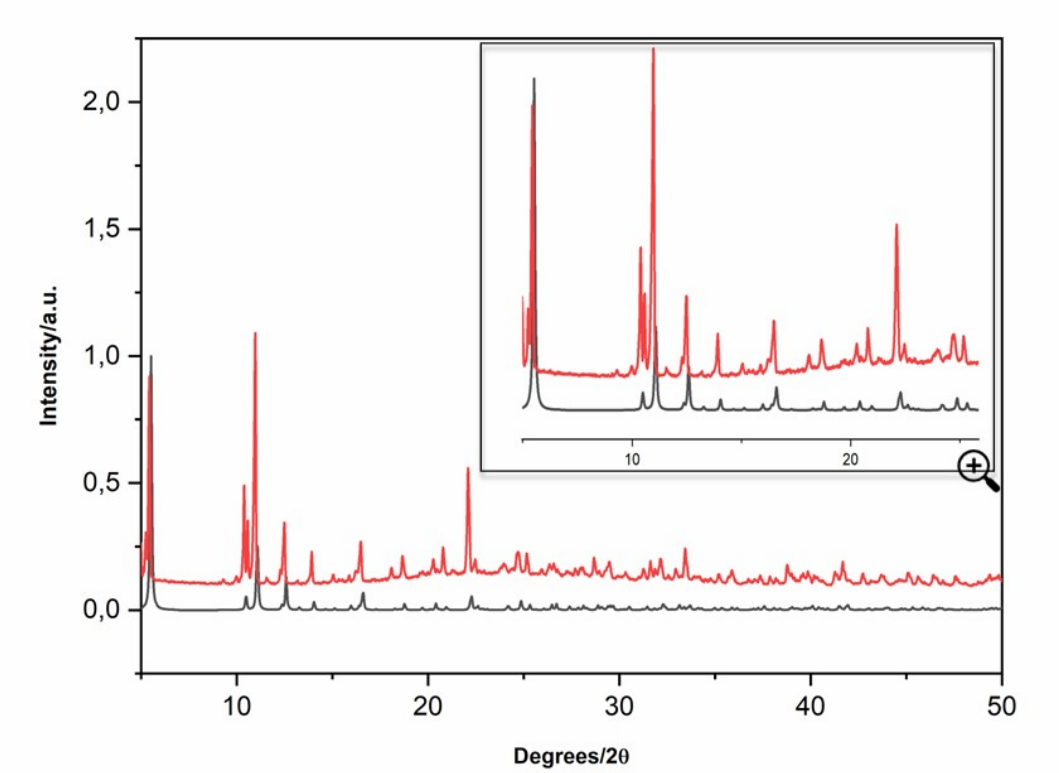

Figure S3. Experimental (red) and calculated (black) PXRD patterns for **1**. The inset shows an overlay between the patterns for a better comparison.

SHAPE details

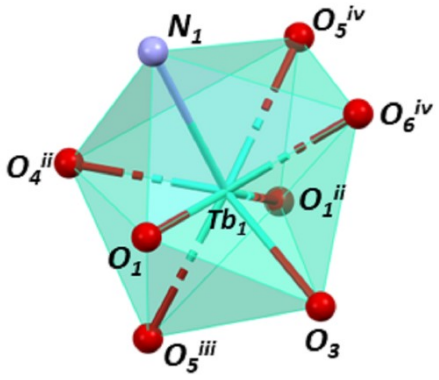

Figure S4. Distorted triangular dodecahedron geometry around the Tb^{III} center in **1**. *Symmetry code*: (ii) = $-x + 3/2, y - 1/2, -z + 1/2$; (iii) $-x + 3/2, -y + 1/2, -z + 1$; (iv) = $x, -y, z - ½$.

Table S3. Geometric analysis of the coordination environment of the terbium(III) ion in **1**, showing the site symmetry approximation derived from continuous shape measures (CShM; via SHAPE[30].

Label	Symmetry	Shape	CShM*
TDD-8	D_{2d}	Triangular dodecahedron	3.162
BTPR-8	C_{2v}	Biaugmented trigonal prism	3.696
JBTPR-8	C_{2v}	Biaugmented trigonal prism J50	3.796
SAPR-8	D_{4d}	Square antiprism	5.324

*The approach is incorporated into the program SHAPE, which is readily available for public use[30]. The values of SHAPE measures relative to other reference polyhedra of **1** are significantly larger. The lower limit corresponds to structures that exactly match the shape of symmetry, and increasing values result in increasingly distorted structures.[31]

Each Tb^{III} ion in **1** is eight-coordinated and its environment has been evaluated as a triangular dodecahedron with a CShM value of 3.162 (Table S3). This geometry also was

observed in the compound $[Dy_4(HL)_2(\mu_3\text{-}OH)_2(piv)_4(MeOH)_2]\cdot 4MeOH\cdot 2H_2O$ (for Dy2) and $[Dy_{21}(L)_7(HL)_7(tfa)_7]Cl_7\cdot 15H_2O\cdot 7MeOH\cdot 12CHCl_3$ (for Dy7)

(H_4L = 6-((bis(2-hydroxyethyl)amino)methyl)-*N'*-((8-hydroxyquinolin-2-yl)methylene)picolinohydrazide; piv = pivalate); tfa =1,1,1-trifluoroacetylacetonate).[32]

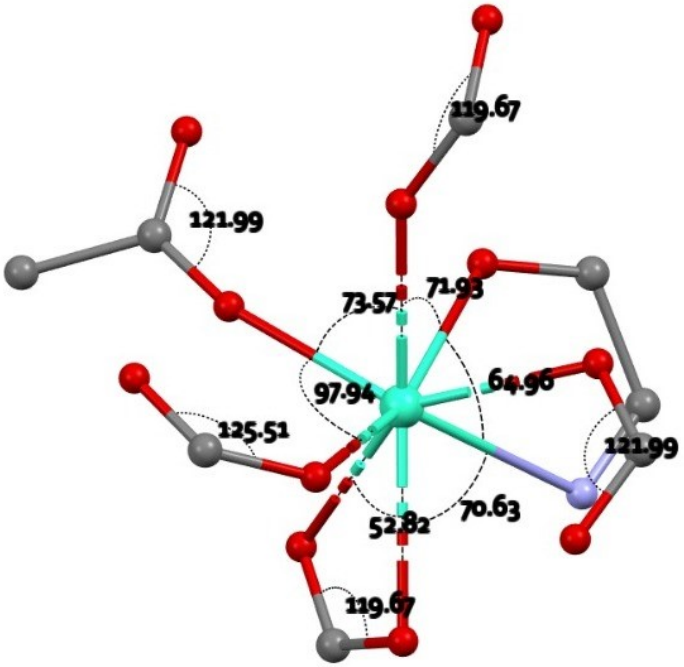

Figure S5. Environment of the terbium(III) ion in **1** showing the values of the O-Tb-O and O-Tb-N bond angles to illustrate their deviations from those of the ideal geometry.

Table S4. C-O bond lengths of $bttb^{4-}$ in **1**.

C-O bond	Bond length (Å)
C_1-O_1	1.288(4)
C_1-O_2	1.198(5)
C_{21}-O_3	1.243(6)
C_{21}-O_4	1.244(6)
C_{20}-O_5	1.273(5)
C_{20}-O_6	1.242(5)

Table S5. Tb^{III} $^5D_4$ state lifetime (298 K, λ_{exc} = 320 nm) calculated from the emission decay curves represented in Figure S7.

Tb^{III} $^5D_4$ state lifetime (ms)	**Average $^5D_4$ state lifetime (ms)**
$\tau_1 = 0.178$ $\tau_2 = 0.736$	$\tau_1 = 0.176$ $\tau_2 = 0.734$
$\tau_1 = 0.179$ $\tau_2 = 0.736$	**Standard deviation**
$\tau_1 = 0.172$ $\tau_2 = 0.732$	0.003 0.002

Table S6. Tb^{III} $^5D_4$ state lifetime (77 K, λ_{exc} = 320 nm) calculated from the emission decay curves represented in Figure S8.

Tb^{III} $^5D_4$ state lifetime (ms)	**Average $^5D_4$ state lifetime (ms)**
$\tau_1 = 0.172$ $\tau_2 = 0.689$	$\tau_1 = 0.174$ $\tau_2 = 0.690$
$\tau_1 = 0.181$ $\tau_2 = 0.696$	**Standard deviation**
$\tau_1 = 0.169$ $\tau_2 = 0.687$	0.006 0.004

Table S7. Tb^{III} $^5D_4$ state (λ_{exc} = 320 nm) and ligand in 400 nm (λ_{exc} = 335 nm) time-dependent lifetime calculated from the emission decay curves represented in Figure S11.

Temperature/ K	Time/ ms (Tb^{III}_{545})	Time/ ns (L_{400})
10	τ_1 = 0.67 ± 0.026	τ_1 = 0.269 ± 0,01
	τ_2 = 0.77 ± 0.01	τ_2 = 1.88 ± 0.043
20	τ_1 = 0.719 ± 0.077	τ_1 = 0.269 ± 0.0123
	τ_2 = 0.756 ± 0.005	τ_1 =2.15667 ± 0.400
40	τ_1 = 0.769 ± 0.075	τ_1 = 0.235 ± 0.014
	τ_2 = 0.743 ± 0.011	τ_1 =2.51333 ± 0.547
60	τ_1 = 0.779 ± 0.067	τ_1 = 0.229 ± 0.004
	τ_2 = 0.736 ± 0.005	τ_2 = 2.58 ± 0.566
80	τ_1 = 0.819 ± 0.097	τ_1 = 0.228 ± 0.008
	τ_2 = 0.733 ± 0.005	τ_2 = 3.11 ± 1.045
100	τ_1 = 0.749 ± 0.093	τ_1 = 0.213 ± 0.006
	τ_2 = 0.726 ± 0.005	τ_2 = 2.443 ± 0.560
120	τ_1 = 0.747 ± 0.069	τ_1 = 0.212 ± 0.011
	τ_2 = 0.726 ± 0.005	τ_2 = 2.443 ± 0.490
140	τ_1 = 0.647 ± 0.041	τ_1 = 0.222 ± 0.009
	τ_2 = 0.73 ± 0	τ_2 = 1.92 ± 0.144
160	τ_1 = 0.578 ± 0.056	τ_1 = 0.214 ± 0.001
	τ_2 = 0.72 ± 0	τ_2 = 1.75 ± 0.166
180	τ_1 = 0.560 ± 0.018	τ_1 = 0.224 ± 0.021
	τ_2 = 0.723 ± 0.011	τ_2 = 1.713 ± 0.066
200	τ_1 = 0.585 ± 0.052	τ_1 = 0.211 ± 0.01
	τ_2 = 0.716 ± 0.005	τ_2 = 1.81 ± 0.185
220	τ_1 = 0.528 ± 0.062	τ_1 = 0.219 ± 0.018
	τ_2 = 0.72 ± 0.01	τ_2 = 1.64 ± 0.165
240	τ_1 = 0.508 ± 0.022	τ_1 = 0.194 ± 0.008
	τ_2 = 0.706 ± 0.004	τ_2 = 1.61333 ± 0.070
260	τ_1 = 0.524 ± 0.053	τ_1 = 0.193 ± 0.003
	τ_2 = 0.713 ± 0.005	τ_2 = 1.57333 ± 0.023
280	τ_1 = 0.465 ± 0.021	τ_1 = 0.204 ± 0.113
	τ_2 = 0.736 ± 0.005	τ_2 = 1.51 ± 0.079
300	τ_1 = 0.476 ± 0.016	τ_1 = 0.249 ± 0.057
	τ_2 = 0.74667 ± 0.020	τ_2 = 1.58 ± 0.0556
320	τ_1 = 0.427 ± 0.021	τ_1 = 0.258 ± 0.028
	τ_2 = 0.723 ± 0.011	τ_2 = 1.44 ± 0.0818

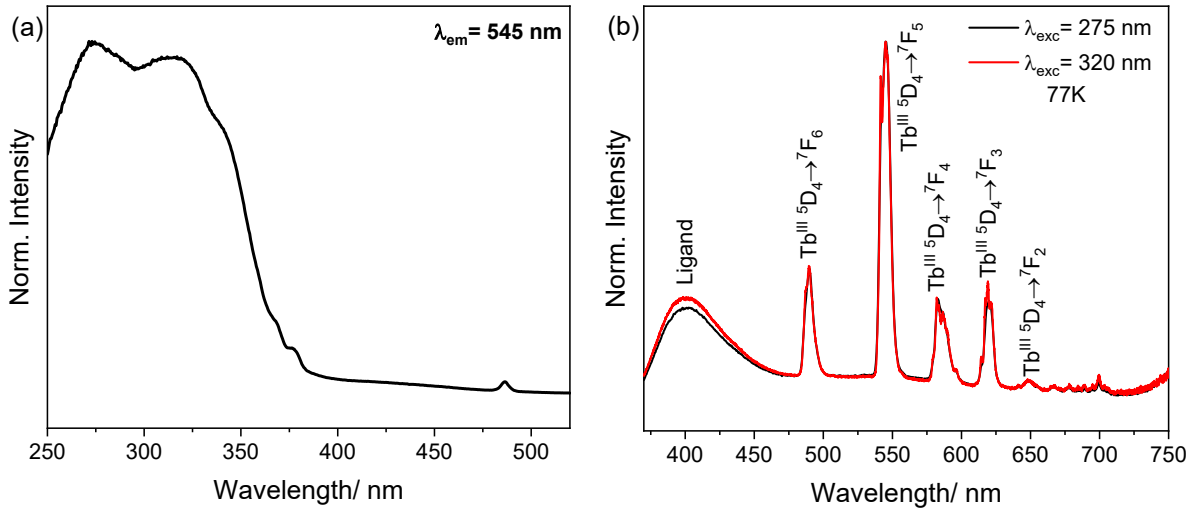

Figure S6 (a) Excitation (λ_{em} = 545 nm) and (b) emission (λ_{exc} = 275 and 320 nm) spectra of **1** monitored at 77 K.

In addition, the data are shown in Tables S5 and S6 [Figures S7 and S8)] show the Tb^{III} lifetime emission of the $^5D_4$ emitting state at two different temperatures (298 K and 77 K). The results illustrate that its luminescent properties stay prominent even through temperature variation.

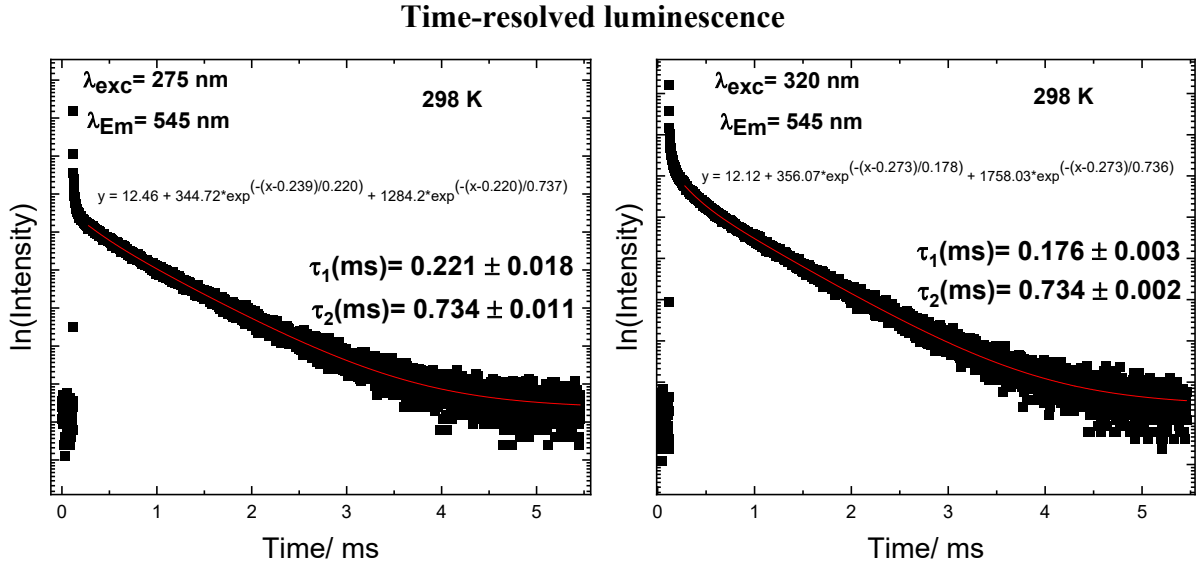

Figure S7. Intensity decay curves for **1** which were obtained with λ_{exc} = 275 or 320 nm and, λ_{em} = 545 nm, at 298 K.

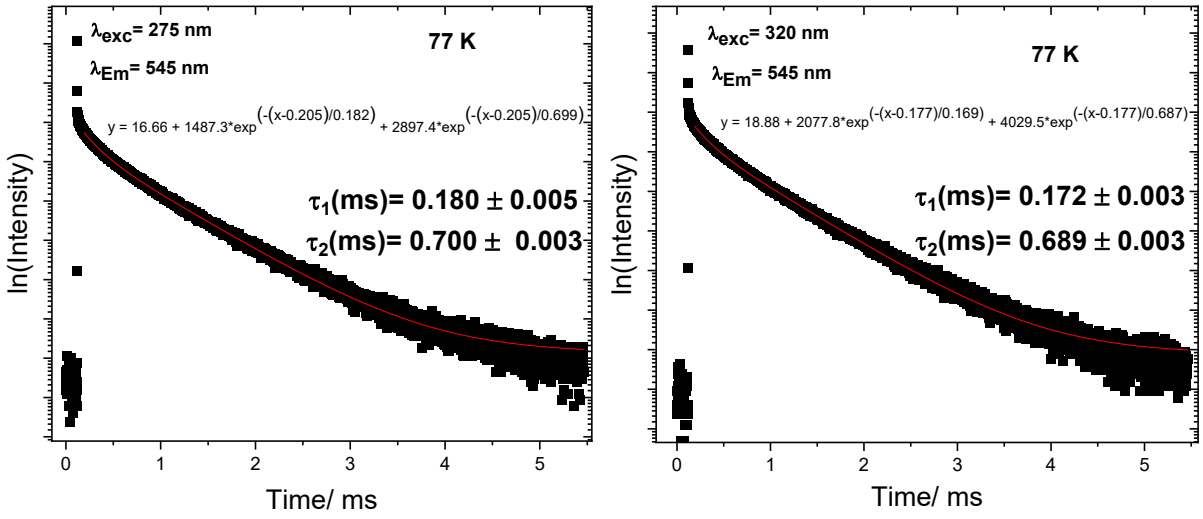

Figure S8. Intensity decay curves for **1** which were obtained with λ_{exc} = 275 or 320 nm and λ_{em} = 545 nm at 77 K.

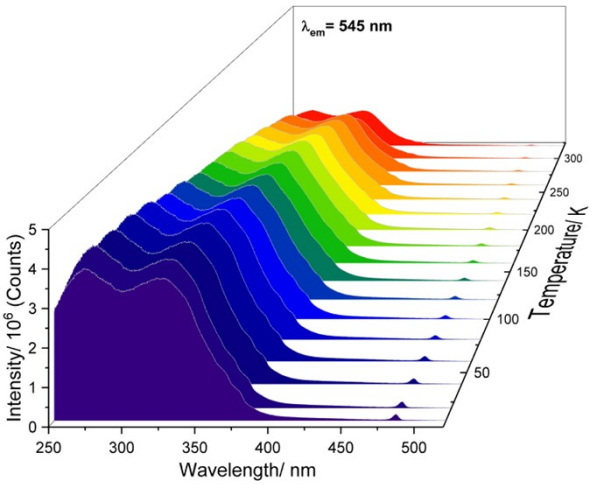

Figure S9. Excitation spectra of **1** at λ_{em}= 545 nm for temperature-dependent luminescent.

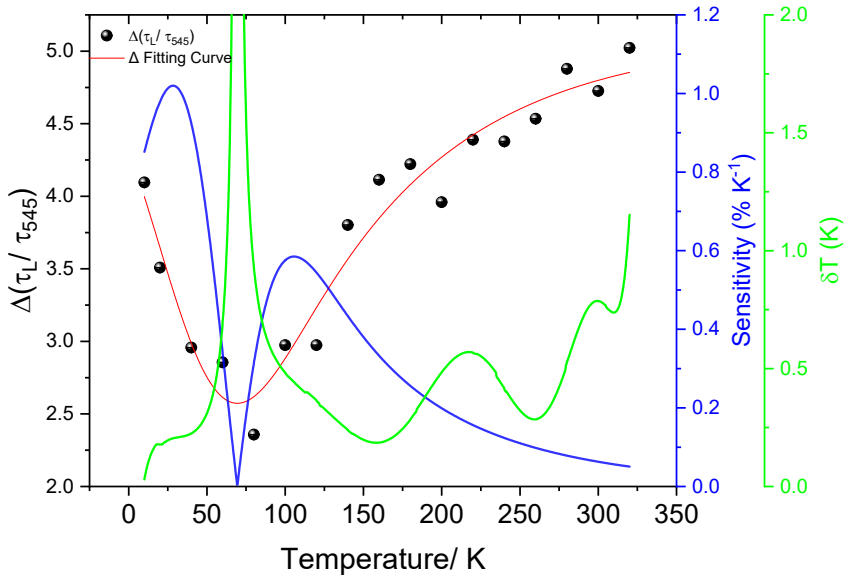

Figure S10. Temperature dependence of the thermometric parameter (Δ), relative thermal sensitivity (S_r), and temperature uncertainty (δT) by considering the thermometric parameter as $\Delta\tau_{400(L)/}\,\tau_{545(Tb)}$ using their longer emission lifetimes.

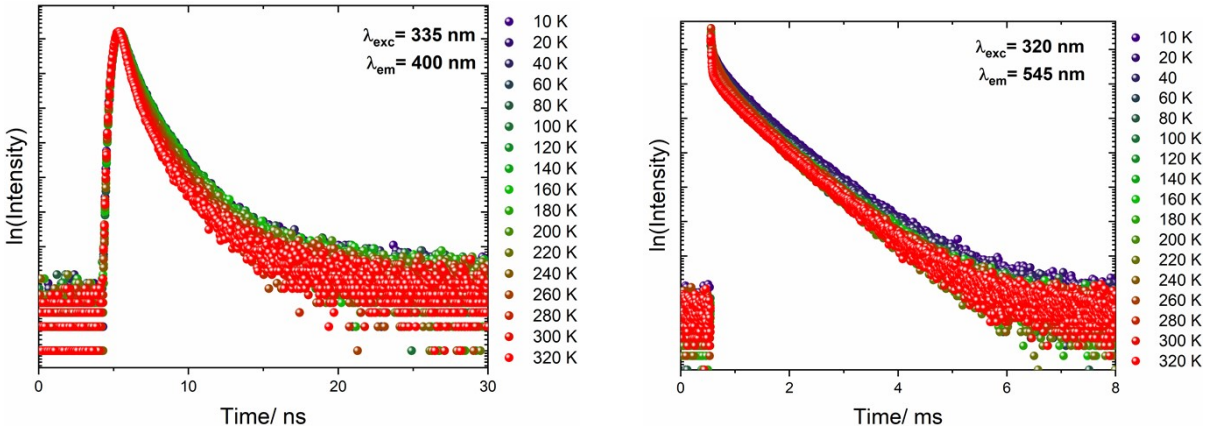

Figure S11. Emission decay curves of (a) the ligand at 400 nm and (b) the $^5D_4$ state (monitoring $^5D_4 \rightarrow {}^7F_5$ at 545 nm) at temperatures below 320 K.

REFERENCES

(1) J. R. Karra, Y. G. Huang, K. S. Walton, *Cryst. Growth Des.* 2013, **13**, 1075–1081.

(2) H. Jasuja, Y. Jiao, N. C. Burtch, Y. G. Huang, K. S. Walton, *Langmuir* 2014, **30**, 14300–14307.

(3) J. E. Warren, C. G. Perkins, K. E. P. Jelfs, P. Boldrin, P. A. Chater, G. J. Miller, T. D. Manning, M. E. Briggs, K. C. Stylianou, J. B. Claridge, M. J. Rosseinsky, *Angew. Chem., Int. Ed.* 2014, **53**, 4592–4596.

(4) I. Burneo, K. C. Stylianou, S. Rodríguez-Hermida, J. X. Juanhuix, Fontrodona, I. Imaz, D. Maspoch, *Cryst. Growth Des.* 2015, **15**, 3182–3189.

(5) X. Chen, A. M. Plonka, D. Banerjee, R. Krishna, H. T. Schaef, S. Ghose, P. K. Thallapally, J. B. Parise, *J. Am. Chem. Soc.* 2015, **137**, 22, 7007–7010.

(6) Z. Guo, D. K. Panda, K. Maity, D. Lindsey, T.G. Parker, T. E. Albrecht-Schmitt, J. L. Barreda-Esparza, P. Xiong, W. Zhou, S. Saha, *J. Mater. Chem. C. Mater.* 2016, **4**, 894–899.

(7) J. R. Karra, H. Jasuja, Y.G. Huang, K.S. Walton, *J. Mater. Chem. A. Mater.* 2015, **3**, 1624–1631.

(8) W. Cheng, T. Wang, W. Xu, Y. Zhang, J. Zhang, M. Fang, *J. Coord. Chem.* 2016, **69**, 2220–2230.

(9) M. Lammert, H. Reinsch, C.A. Murray, M.T. Wharmby, H. Terraschke, N. Stock, *Dalton Trans.* 2016, **45**, 18822–18826.

(10) A. M. Plonka, X. Chen, H. Wang, R. Krishna, X. Dong, D. Banerjee, W. R. Woerner, Y. Han, J. Li, J. B. Parise, *Chem. Mat.* 2016, **28**, 1636–1646.

(11) F. Yuan, C. Yuan, H. Hu, T. Wang, C. Zhou, *Polyhedron* 2018, **139**, 257–261.

(12) R. G. Abdulhalim, P. M. Bhatt, Y. Belmabkhout, A. Shkurenko, K. Adil, L.J. Barbour, M. Eddaoudi, *J. Am. Chem. Soc.* 2017, **139**, 10715–10722.

(13) M. Y. Tsang, S. Rodríguez-Hermida, K. C. Stylianou, F. Tan, D. Negi, F. Teixidor, C. Viñas, D. Choquesillo-Lazarte, C. Verdugo-Escamilla, M. Guerrero, J. Sort, J. Juanhuix, D. Maspoch, J. G. Planas, *Cryst. Growth Des.* 2017, **17**, 846–857.

(14) F. Yuan, C. M. Yuan, H. M. Hu, T.T. Wang, C.S. Zhou, *Polyhedron* 2018, **139**, 257–261.

(15) M. Köppen, V. Meyer, J. Ångström, A. K. Inge, N. Stock, *Cryst. Growth Des.* 2018, **18**, 4060–4067.

(16) D. Banerjee, X. Chen, S.S. Lobanov, A.M. Plonka, X. Chan, J.A. Daly, T. Kim, P.K. Thallapally, J. B. Parise, *ACS Appl. Mater. Interfaces* 2018, **10**, 10622–10626.

(17) S. S. Dhankhar, C.M. Nagaraja, *New J. Chem.* 2019, **43**, 2163–2170.

(18) S. E. Gilson, P. Li, J. E. S. Szymanowski, J. White, D. Ray, L. Gagliardi, O.K. Farha, P. C. Burns, *J. Am. Chem. Soc.* 2019, **141**, 11842–11846.

(19) P. Rönfeldt, H. Reinsch, M.P.M. Poschmann, H. Terraschke, N. Stock, *Cryst. Growth Des.* 2020, **20**, 4686–4694.

(20) N. Dissem, M. Essalhi, N. Ferhi, A. Abidi, T. Maris, A. Duong, *Dalton Trans.* 2021, **50**, 8727–8735.

(21) H.Q. Yin, K. Tan, S. Jensen, S. J. Teat, S. Ullah, X. Hei, E. Velasco, K. Oyekan, N. Meyer, X.Y. Wang, T. Thonhauser, X. B. Yin, J. Li, *Chem. Sci.* 2021, **12**, 14189–14197.

(22) D. H. Le, R.P. Loughan, A. Gładysiak, N. Rampal, I. A. Brooks, A.H.A. Park, D. Fairen-Jimenez, K.C. Stylianou, *J. Mater. Chem. A. Mater.* 2022, **10**, 1442–1450.

(23) D. F. Sava Gallis, K.S. Butler, C. J. Pearce, N. Valdez, M. A. Rodriguez, *ACS Appl. Mater. Interfaces* 2022, **14**, 10566–10576.

(24) B. C. Chen, C. Q. Xiao, J. J. Hu, Y. Peng, H. R. Wen, S. J. Liu, *Inorg. Chem.* 2023, **62**, 6255-6262.

(25) J. Z. Gu, Z. Q. Gao, *J. Chem. Crystallogr.* 2012, **42**, 283–289.

(26) Y. Pan, D. Ma, H. Liu, H. Wu, D. He, Y. Li, *J. Mater. Chem*. 2012, **22**, 10834–10839.

(27) J. Cepeda, S. Pérez-Yáñez, G. Beobide, O. Castillo, J.Á. García, A. Luque, *Eur. J. Inorg. Chem.* 2015, **2015**, 4318–4328.

(28) M. V. Marinho, D. O. Reis, W.X.C. Oliveira, L.F. Marques, H.O. Stumpf, M. Déniz, J. Pasán, C. Ruiz-Pérez, J. Cano, F. Lloret, M. Julve. *Inorg. Chem.* 2017, **56**, 2108–2123.

(29) M. O. Barsukova, S. V. Cherezova, A.A. Sapianik, O. V. Lundovskaya, D. G. Samsonenko, V.P. Fedin, *RSC Adv.* 2020, **10**, 38252–38259.

(30) M. Llunell, D. Casanova, J. Cirera, P. Alemany, S. Alvarez, SHAPE: Program for the Stereochemical Analysis of Molecular Fragments by Means of Continuous Shape Measures and Associated Tools, v2.1, Eletronic Structure Group, Universitat de Barcelona. 2013.

(31) S. Alvarez, M. Llunell, *J. Chem. Soc., Dalton Trans.* 2000, 3288–3303.

(32) S. Biswas, S. Das, J. Acharya, V. Kumar, J. van Leusen, P. Kögerler, J.M. Herrera, E. Colacio, V. Chandrasekhar, *Chem. - A Eur. J.* 2017, **23**, 5154–5170.